Identifying Microvascular and Neural Parameters Related to the Severity of Diabetic Retinopathy Using Optical Coherence Tomography Angiography

Xiaoli Li,[1,2] Jie Xie,[1] Liang Zhang,[1] Ying Cui,[1] Guanrong Zhang,[3] Xiangting Chen,[1,4] Jun Wang,[1] Aiping Zhang,[1] Tian Huang,[1,5] and Qianli Meng[1,4,5]

[1]Guangdong Eye Institute, Department of Ophthalmology, Guangdong Provincial People's Hospital, Guangdong Academy of Medical Sciences, Guangzhou, China
[2]Shantou University Medical College, Shantou, China
[3]Information and Statistical Center, Guangdong Provincial People's Hospital, Guangdong Academy of Medical Sciences, Guangzhou, China
[4]School of Medicine, South China University of Technology, Guangzhou, China
[5]The Second School of Clinical Medicine, Southern Medical University, Guangzhou, China

Correspondence: Qianli Meng, Guangdong Eye Institute, Department of Ophthalmology, Guangdong Provincial People's Hospital, Guangdong Academy of Medical Sciences, 106 Zhongshan Er Road, Guangzhou 510080, PR China; mengqly@163.com.

XL and JX contributed equally to this work.

Received: November 12, 2019
Accepted: April 13, 2020
Published: May 22, 2020

Citation: Li X, Xie J, Zhang L, et al. Identifying microvascular and neural parameters related to the severity of diabetic retinopathy using optical coherence tomography angiography. *Invest Ophthalmol Vis Sci.* 2020;61(5):39. https://doi.org/10.1167/iovs.61.5.39

Purpose. To identify microvascular and neural parameters related to the severity of diabetic retinopathy (DR) by using optical coherence tomography angiography in patients with type 2 diabetes.

Methods. This cross-sectional study included 110 eyes (63 patients) with no DR, 46 eyes (33 patients) with mild nonproliferative DR, 36 eyes (23 patients) with moderate nonproliferative DR, 36 eyes (22 patients) with severe nonproliferative DR, and 31 eyes (19 patients) with proliferative DR. The optical coherence tomography angiography images were processed to quantify the foveal avascular zone parameters, macular vessel density (VD), retinal thickness, peripapillary VD, retinal nerve fiber layer thickness, and ganglion cell complex thickness. A LASSO-based continuation ratio model was used to select the most clinically relevant parameters for predicting the stage of DR.

Results. The regression model identified a set of regional parameters for each scanning pattern that identified the DR severity, including foveal avascular zone perimeter; FD-300; temporal perifoveal superficial capillary plexus VD and retinal thickness; temporal and nasal parafoveal deep capillary plexus VD; peripapillary VD in the temporal superior, nasal inferior, and temporal inferior sectors; temporal superior and nasal inferior retinal nerve fiber layer thickness; ganglion cell complex thickness; and FLV, which changed significantly with the progression of DR. Furthermore, two combined blocks exhibited different sensitive parameters to differentiate between the groups based on DR severity. Similar results were obtained in eyes without diabetic macular edema.

Conclusions. We identified microvascular and neural parameters related to the severity of DR using optical coherence tomography angiography, suggesting their potential clinical application for better screening and staging of DR.

Keywords: optical coherence tomography angiography, diabetic retinopathy, microvasculature, neuron, parameters

Diabetic retinopathy (DR) is characterized by structural and functional alterations in the retinal microvasculature, causing capillary occlusion, vascular hyperpermeability, and neovascularization in the retina. Extensive study of diabetic retinal neurodegeneration indicates that DR is additionally a neurodegenerative disease; further, the potential relationship between neurodegeneration and microvascular impairment has been discussed.[1] Recently, macular microvascular changes in DR have been frequently reported in optical coherence tomography angiography (OCTA) studies.[1–15] However, the optic nerve head area and the ganglion cell complex (GCC), which are usually analyzed in glaucoma and optic neuropathy, are not intensively studied in DR.[16,17] Because DR is considered a neurovascular degenerative disease caused by multifactorial and complex mechanisms,[18] studying the characteristics of simultaneous changes in microvasculature and neuron at different stages of DR becomes indispensable and meaningful.

Having emerged as a noninvasive imaging technique without dye injection, OCTA allows for fast visualization of macular vasculature and differentiation of various retinal vascular layers, such as superficial capillary plexus (SCP)

and deep capillary plexus (DCP).[1,4,5,7,10,13,15] Most recent qualitative and quantitative studies on DR using OCTA were focused on structural changes in the foveal avascular zone (FAZ) and the macular retinal microvasculatures,[1–15] and have proposed OCTA as a potential tool for measuring the macular area and for follow-up in patients with DR. In addition, most studies on retinal neurovascular impairment detected by OCTA are focused on preclinical or early DR,[17,19–22] and do not sufficiently consider the changes in both retinal microvasculatures and neurons at all DR stages. Furthermore, even among the lesser number of studies in the literature that are focused on the relationship between the OCTA parameters and the stage of DR,[1,2,8,10,14,15] only a few have attempted to combine these parameters to differentiate eyes with and without DR, or eyes with nonproliferative DR (NPDR) from those with proliferative DR (PDR).[10,13]

Accordingly, the objective of this study is to investigate the change in characteristics from no DR to PDR based on the OCTA parameters in the macular area, optic nerve head area, and GCC. In addition, this study seeks to identify the OCTA parameters that are most related to DR severity to differentiate the stages of DR.

Methods

This prospective, observational, and cross-sectional study complied with the ethical principles of the Declaration of Helsinki, and was approved by the research ethics committee of Guangdong Provincial People's Hospital. In addition, written informed consent was obtained from all participants.

Patients

Patients with type 2 diabetes mellitus who underwent OCTA at the Department of Ophthalmology at Guangdong Provincial People's Hospital between June 2018 and January 2019, were included. DR was evaluated and categorized into no DR, mild NPDR, moderate NPDR, severe NPDR, and PDR based on clinical assessments by two experienced ophthalmologists (QM and JW) using the proposed international DR severity scale.[23,24] Diabetic macular edema (DME) was confirmed by optical coherence tomography (OCT). The exclusion criteria included media opacities, coexistence of other retinal diseases, glaucoma or ocular hypertension, axial length (AL) shorter than 20.0 mm or longer than 27.0 mm, history of ophthalmic intervention procedure (e.g., laser photocoagulation, anti-vascular endothelial growth factor intravitreal injection, and vitrectomy), and low-quality OCTA images (e.g., quality index of ≤60, blink artifacts, poor fixation leading to motion or doubling artifacts, and/or segmentation errors).

Ophthalmic Examinations

All participants underwent a comprehensive ophthalmic examination, including best-corrected visual acuity, intraocular pressure measurement, slit-lamp examination, dilated fundoscopy, nine fields of 45° color fundus photography (TRC-NW8 fundus camera, TOPCON, Tokyo, Japan), ocular biometry (LS900, Haag-Streit, Köniz, Switzerland), OCT (HRA-OCT, Heidelberg Engineering, Jena, Germany), and OCTA (Optovue, Fremont, CA, USA). Fundus fluorescein angiography (Spectralis HRA, Heidelberg Engineering) was performed on the patients with moderate NPDR, severe NPDR, and PDR.

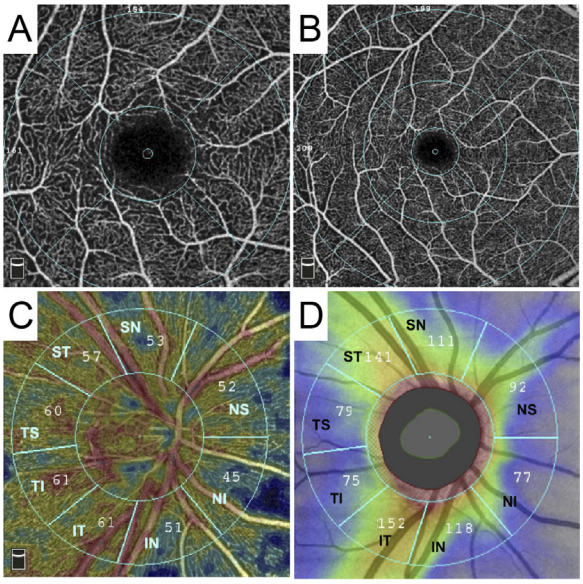

Figure 1. Angio retina and disc measurement zones. (**A**) A 3.0 mm scan centered on the fovea at the SCP. (**B**) A 6.0 mm scan centered on the fovea at the SCP. The Early Treatment Diabetic Retinopathy Study grid in the macular area comprises 2 (3.0 mm scan) or 3 (6.0 mm scan) concentric rings: 1 mm center (fovea), 1 to 3 mm (parafovea), and outer ring of 3 to 6 mm diameters (perifovea). The outermost rings in both 3.0 mm and 6.0 mm scans are further divided into four sectors (temporal [T], superior [S], nasal [N], and inferior [I]) or two hemispheres (superior hemisphere and inferior hemisphere) divided by a horizontal line through the foveal center. (**C**) Peripapillary VD. (**D**) Peripapillary retinal thickness. Peripapillary region at 4.5 mm scan is defined by two rings of 2 mm and 4 mm centered on the disc center. The modified eight peripapillary sectors grid aims to follow RNFL distribution and sectored to provide easier correlation with the visual field. The eight peripapillary sectors include nasal superior (NS), nasal inferior (NI), inferior nasal (IN), inferior temporal (IT), temporal inferior (TI), temporal superior (TS), superior temporal (ST), and superior nasal (SN).

OCTA Image Acquisition and Analysis

The OCTA images were obtained using the split-spectrum amplitude decorrelation angiography algorithm incorporated with the RTVue-XR Avanti device with Angio Vue 2.0.[25] Angio Retina 3.0 mm and HD Angio Retina 6.0 mm scans centered on the fovea, HD Angio Disc 4.5 mm scan centered on the disc, and GCC scan focused on the ganglion cells were used in this study. All OCTA scans were performed by a single experienced examiner, and the obtained images were individually reviewed by two investigators (XL and JX) for quality evaluation. Further, individual AL was obtained using LS900 to correct the retinal magnification of each OCTA image.

Vessel Density and Retinal Thickness. A vessel density (VD) map is used to assess the relative density of flow as a percentage of the total area. With the assistance of en face OCT angiograms, SCP is defined as a slab extending from the internal limiting membrane to 10 µm above the inner plexiform layer, and DCP as a slab extending from 10 µm above the inner plexiform layer to 10 µm below the outer plexiform layer. Macular VD is distinctly evaluated from both SCP and DCP within the Early Treatment Diabetic Retinopathy Study 3 × 3 whole grid or 6 × 6 whole grid (Figs. 1A and 1B). The peripapillary VD and the retinal nerve fiber layer (RNFL) thickness are quantified in the

Investigative Ophthalmology & Visual Science

Table 1. Demographics and Ocular Biometric Characteristics for Patients With Different Stages of DR

Variables	Stages of DR					*P* value
	NDR	Mild NPDR	Moderate NPDR	Severe NPDR	PDR	
Total number (eyes)	110	46	36	36	31	
DME number (eyes)	0	0	5	15	7	
Age (years)	56.94 ± 12.43	58.17 ± 9.47	63.08 ± 7.74	55.64 ± 10.65	52.45 ± 8.98	0.002
Sex (male/female)	42/21	22/11	10/13	12/10	8/11	0.134
AL (mm)	23.68 ± 0.95	23.59 ± 0.92	23.19 ± 0.82	23.34 ± 1.00	22.47 ± 0.75	<0.001
SFCT (μm)	260.97 ± 73.94	249.15 ± 79.18	275.50 ± 63.20	259.50 ± 55.59	274.97 ± 12.50	0.41
3.0 mm scan						
FAZ area (mm^2)	0.31 ± 0.12	0.33 ± 0.14	0.37 ± 0.13	0.38 ± 0.15	0.37 ± 0.15	<0.001
Whole SCP VD (%)	45.85 ± 3.92	45.22 ± 3.23	43.07 ± 3.68	38.36 ± 4.64	38.35 ± 4.69	<0.001
Whole DCP VD (%)	49.93 ± 3.71	49.76 ± 4.09	46.18 ± 3.23	43.06 ± 3.93	42.24 ± 5.73	<0.001
Central foveal thickness (μm)	245.61 ± 19.51	245.46 ± 20.72	255.94 ± 41.44	311.56 ± 107.34	339.12 ± 180.75	<0.001
Whole retinal thickness (μm)	313.70 ± 18.39	311.00 ± 11.86	319.25 ± 23.00	365.50 ± 67.95	376.12 ± 112.94	<0.001
6.0 mm scan						
FAZ area (mm^2)	0.29 ± 0.11	0.32 ± 0.14	0.37 ± 0.16	0.38 ± 0.14	0.43 ± 0.23	<0.001
Whole SCP VD (%)	48.77 ± 3.75	48.59 ± 3.52	46.55 ± 3.32	43.90 ± 4.95	44.34 ± 5.41	<0.001
Whole DCP VD (%)	49.36 ± 5.46	49.34 ± 5.73	45.70 ± 5.33	43.88 ± 4.94	42.08 ± 4.63	<0.001
Central foveal thickness (μm)	245.92 ± 19.17	245.59 ± 20.99	256.74 ± 42.86	309.12 ± 99.37	345.35 ± 207.12	<0.001
Whole retinal thickness (μm)	285.54 ± 17.16	283.43 ± 12.15	293.00 ± 16.56	332.35 ± 43.41	347.06 ± 93.38	<0.001
Whole peripapillary VD (%)	52.08 ± 3.21	51.77 ± 6.65	50.63 ± 3.24	48.64 ± 3.25	46.08 ± 5.65	<0.001
Peripapillary RNFL thickness (μm)	118.55 ± 14.28	113.25 ± 11.75	113.92 ± 10.83	125.31 ± 29.85	129.12 ± 28.99	<0.001
Total GCC thickness (μm)	100.05 ± 7.62	99.73 ± 7.17	104.68 ± 10.28	122.35 ± 22.87	139.74 ± 61.13	<0.001

Values are number or mean ± standard deviation.
NDR, no DR; SD, stand deviation; SFCT, subfovea choroidal thickness.

radial peripapillary capillary segment, which is defined as a slab extending from internal limiting membrane to RNFL. The area is divided into different sections, as shown in Figures 1C and 1D.

FAZ Parameters. The FAZ parameters were evaluated using the nonflow area tool to provide automated FAZ segmentation, including FAZ area, FAZ perimeter, acircularity index (AI), and FD-300. Acircularity represents the extent to which FAZ differs from a perfect circle, with the value of 1.0 representing a perfect circle.[14] FD-300 is a parameter that shows the capillary density from internal limiting membrane to outer plexiform layer in a 300 μm wide region around FAZ.

GCC Parameters. A GCC scan is used to measure the thickness of the retinal GCC of diameter 6 mm, including the RNFL, ganglion cell layer, and inner plexiform layer. Further, the GCC thickness, focal loss volume (FLV), and global loss volume are automatically calculated. The FLV quantifies the amount of significant GCC loss, which is expressed as a percentage of the map with significant ganglion cell loss. The global loss volume quantifies the total amount of GCC loss over the entire GCC map, which is a sum of the pixels (where the fractional deviation map value is < 0) divided by the total map area, to provide a percentage loss of GCC thickness.

Statistical Analysis

All statistical analyses were performed using the SPSS statistical software (version 21.0) and R software (version 3.5.1). Continuous variables were presented as mean ± standard deviation, and sex was compared using a χ^2 test. The AL, subfoveal choroidal thickness, and OCTA parameters in patients with different stages of DR were compared using one-way ANOVA. Data preprocessing, including log transformation, standardization, and normalization, was applied to all ophthalmic variables before constructing DR classification models. Penalized constrained continuation ratio models were fitted to individual block and combined block of OCTA image parameters using the glmnetcr package, an adaption of the LASSO regularization method. The final multivariate model was selected according to the minimum Bayesian information criterion. Ordinal logistic regression was performed to estimate the relationships between selected variables and stage of DR. Differences were considered to be statistically significant at a *P* value of less than 0.05.

Results

A total of 259 eyes (136 participants: 78 males and 58 females) were analyzed, which included 110 eyes (63 patients) with no DR, 46 eyes (33 patients) with mild NPDR, 36 eyes (23 patients) with moderate NPDR, 36 eyes (22 patients) with severe NPDR, and 31 eyes (19 patients) with PDR. Table 1 presents the demographics and the ocular biometric characteristics for patients with different stages of DR. The age and AL were significantly different at each stage of DR. In both the 3.0 mm and 6.0 mm scans, FAZ area, central foveal thickness and whole retinal thickness significantly increased, whereas whole SCP and DCP VD significantly decreased with the progression of DR.

Using LASSO regularization, six sensitive parameters related to the severity of DR were identified from 37 parameters in the 3.0 mm scan; similarly, eight sensitive parameters from 58 parameters in 6.0 mm scan, five sensitive parameters from 16 parameters in 4.5 mm scan, and two sensitive parameters from five parameters in the GCC scan were identified (Table 2). All the identified sensitive parameters had significantly statistical differences between each stage of DR (Supplementary Table S1).

The odds ratios (OR) of selected parameters with DR stage were estimated using the ordinal logistic regression

Investigative Ophthalmology & Visual Science

Table 2. LASSO Regularization Identified OCTA Parameters Related to the Severity of DR

Dataset	Total No. of Parameters	No. of Identified Parameters	Identified Parameters
A. 3.0 mm scan			
FAZ metrics	4	2	FAZ perimeter, FD-300
Macular VD	22	3	Inferior hemisphere SCP VD, temporal parafoveal DCP VD, nasal parafoveal DCP VD
Retinal thickness	11	1	Superior hemisphere foveal thickness
B. 6.0 mm scan			
FAZ metrics	4	3	FAZ perimeter, FD-300, AI
Macular VD	36	4	Temporal perifoveal SCP VD, Foveal DCP VD, temporal parafoveal DCP VD, nasal parafoveal DCP VD
Retinal thickness	18	1	Temporal perifoveal thickness
C. 4.5 mm scan			
Peripapillary VD and RNFL thickness	16	5	Temporal superior peripapillary VD, nasal inferior peripapillary VD, temporal inferior peripapillary VD, temporal superior RNFL thickness, nasal inferior RNFL thickness
D. GCC scan	5	2	Total GCC thickness, FLV
Combination 1			
A+C+D	58	6	FAZ perimeter, inferior hemisphere SCP VD, temporal parafoveal DCP VD, temporal superior peripapillary VD, total GCC thickness, FLV
Combination 2			
B+C+D	79	7	Temporal perifoveal SCP VD, foveal DCP VD, temporal parafoveal DCP VD, temporal perifoveal thickness, temporal superior peripapillary VD, total GCC thickness, FLV

Table 3. Ordered Multiclass Logistic Regression Model for the Most Parsimonious Parameters Related to the Severity of DR in Individual Blocks

Parameters*	OR Value	Standard Error	*P* Value
A. 3.0 mm scan			
FAZ perimeter	13.02	2.27	<0.001
FD-300	−14.59	2.18	<0.001
Inferior hemisphere SCP VD	−13.38	2.55	<0.001
Temporal parafoveal DCP VD	−10.70	3.63	0.002
Nasal parafoveal DCP VD	−7.72	3.37	0.024
Superior hemisphere foveal thickness	14.50	2.30	<0.001
B. 6.0 mm scan			
FAZ perimeter	10.71	2.89	<0.001
AI	7.32	3.71	0.03
FD-300	−7.66	2.14	<0.001
Temporal perifoveal SCP VD	−8.51	2.23	<0.001
Foveal DCP VD	−4.33	2.17	0.046
Temporal parafoveal DCP VD	−8.50	2.83	0.002
Nasal parafoveal DCP VD	−7.25	2.77	0.007
Temporal perifoveal thickness	21.64	2.76	<0.001
C. 4.5 mm scan			
Temporal superior peripapillary VD	−9.78	2.33	<0.001
Nasal inferior peripapillary VD	−7.56	2.23	<0.001
Temporal inferior peripapillary VD	−5.47	2.37	0.021
Temporal superior RNFL thickness	7.43	2.37	<0.001
Nasal inferior RNFL thickness	5.43	2.40	0.022
D. GCC scan			
Total GCC thickness	27.42	3.16	<0.001
FLV	13.72	2.46	<0.001

* Adjusting for age, sex, and AL. OR, odds ratio.

model within each individual block (Table 3) and combined block (Table 4) after adjusting for age, sex, and AL. As shown in Table 3, in 3.0 mm scans, FAZ perimeter (OR, 13.02; $P < 0.001$) and superior hemisphere foveal thickness (OR, 14.5; $P < 0.001$) were significantly high, whereas FD-300 (OR, –14.59; $P < 0.001$), inferior hemisphere SCP VD (OR, –13.38; $P < 0.001$), and temporal (OR, –10.70; $P = 0.002$) and nasal (OR, –7.72; $P = 0.024$) parafoveal DCP VD were significantly low with the progression of DR (Figs. 2A–2D). In the 6.0 mm scan, FAZ perimeter (OR, 10.71; $P < 0.001$), AI (OR, 7.32; *P*

Investigative Ophthalmology & Visual Science

Table 4. Ordered Multiclass Logistic Regression Model for the Most Parsimonious Parameters Related to the Severity of DR in Combined Blocks

Parameter*	OR Value	Standard Error	*P* Value
Combination 1			
FAZ perimeter	6.84	2.34	0.003
Inferior-hemisphere SCP VD	−12.18	2.80	<0.001
Temporal parafoveal DCP VD	−10.11	2.98	<0.001
Temporal superior peripapillary VD	−5.22	2.53	0.034
Total GCC thickness	17.46	3.05	<0.001
FLV	5.92	2.50	0.017
Combination 2			
Temporal perifoveal SCP VD	−8.37	2.38	<0.001
Foveal DCP VD	−5.64	2.36	0.016
Temporal parafoveal DCP VD	−6.15	2.53	0.014
Temporal perifoveal thickness	11.73	4.10	0.003
Temporal superior peripapillary VD	−7.01	2.33	0.002
Total GCC thickness	13.51	4.19	0.001
FLV	7.15	2.58	0.005

* Adjusting for age, sex, and AL. OR, odds ratio.

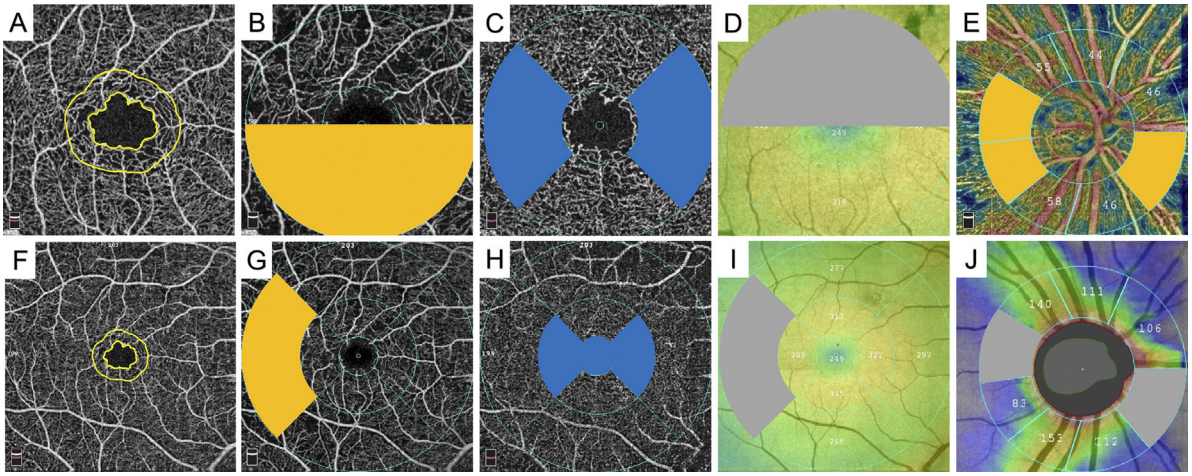

Figure 2. Schematic presentation illustrating the parsimonious parameters in an individual block on OCTA images at different scans. (**A–D**): A 3.0 mm scan. (**A**) FAZ perimeter and FD-300 (*yellow ring*). (**B**) Inferior hemisphere SCP VD (*yellow*). (**C**) Temporal and nasal parafoveal DCP VD (*blue*). (**D**) Superior hemisphere foveal thickness (*gray*). (**F–I**) A 6.0 mm scan. (**F**) FAZ perimeter and FD-300 (*yellow ring*). (**G**) Temporal perifoveal SCP VD (*yellow*). (**H**) Foveal, temporal and nasal parafoveal DCP VD (*blue*). (**I**) Temporal perifoveal thickness (*gray*). (**E** and **J**) A 4.5 mm scan. (**E**) Temporal superior, nasal inferior and temporal inferior peripapillary VD (*yellow*). (**J**) Temporal superior and nasal inferior RNFL thickness (*gray*).

= 0.04), and temporal perifoveal thickness (OR, 21.64; $P <$ 0.001) significantly increased, whereas FD-300 (OR, –7.66; $P <$ 0.001), temporal perifoveal SCP VD (OR, –8.51; $P <$ 0.001), foveal DCP VD (OR, –4.33; $P =$ 0.02), and temporal (OR, –8.50; $P =$ 0.046) and nasal (OR, –7.25; $P =$ 0.007) parafoveal DCP VD significantly decreased with the worsening of the DR stage (Figs. 2F–2I). In the 4.5 mm scan, temporal superior (OR, –9.78; $P <$ 0.001), nasal inferior (OR, –7.56; $P <$ 0.001), and temporal inferior (OR, –5.47; $P =$ 0.021) peripapillary VD significantly decreased, whereas temporal superior (OR, 7.43; $P <$ 0.001) and nasal inferior RNFL thickness (OR, 5.43; $P =$ 0.022) significantly increased with the increase in DR severity (Figs. 2E and 2J). Further, a significant increase in total GCC thickness (OR, 27.42; $P <$ 0.001) and FLV (OR, 13.72; $P <$ 0.001) was observed with the progression of DR. Figure 3 shows the representative OCTA images of eyes with different stages of DR.

Table 4 summarizes the results of the combined blocks. With the progression of DR, a significant increase in FAZ perimeter (OR, 6.84; $P =$ 0.003), total GCC thickness (OR, 17.46; $P <$ 0.001), and FLV (OR, 5.92; $P =$ 0.017), and a significant decrease in VD in inferior hemisphere SCP (OR, -12.18; $P <$ 0.001), temporal parafoveal DCP (OR, -10.11; $P <$ 0.001), and temporal superior peripapillary sector (OR, –5.22; $P =$ 0.034), were found in combination 1 (Figs. 4A–4D, 4H). In combination 2, VD in temporal perifoveal SCP (OR, –8.37; $P <$ 0.001), foveal DCP (OR, –5.64; $P =$ 0.016), temporal parafoveal DCP (OR, –6.15; $P =$ 0.014), and temporal superior peripapillary sector (OR, –7.01; $P =$ 0.002) significantly decreased, whereas temporal perifoveal thickness (OR, 11.73; $P =$ 0.003), total GCC thickness (OR, 13.51; $P =$ 0.001), and FLV (OR, 7.15; $P =$ 0.005) significantly increased with the increase in DR severity (Figs. 4D–4H).

In addition, considering that DME could naturally result in the increase of retinal and GCC thickness with the progression of DR, we further analyzed the demographics, ocular biometric characteristics and OCTA parameters in patients without DME (Supplementary Tables S2 to S5). The

Investigative Ophthalmology & Visual Science

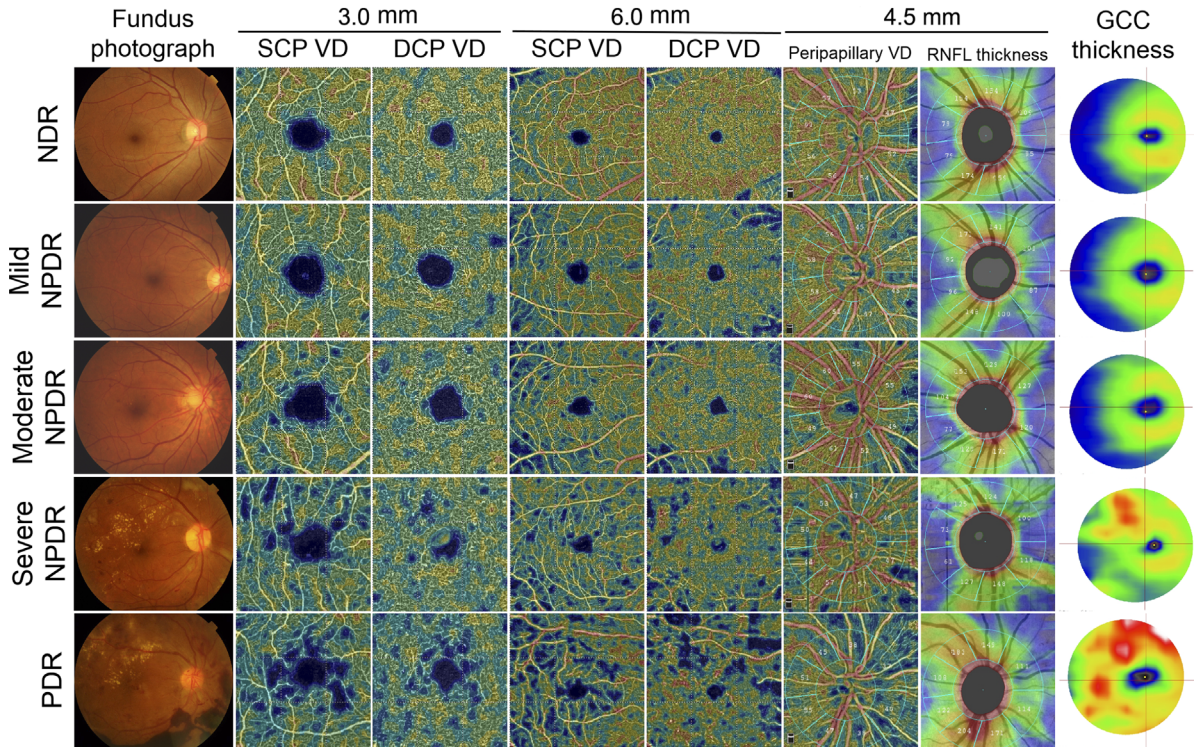

Figure 3. Representative OCTA images of eyes with different stages of DR at the 3.0 mm and 6.0 mm scans for macular VD in SCP and DCP, and 4.5 mm scan for peripapillary VD and RNFL thickness. NDR, no DR.

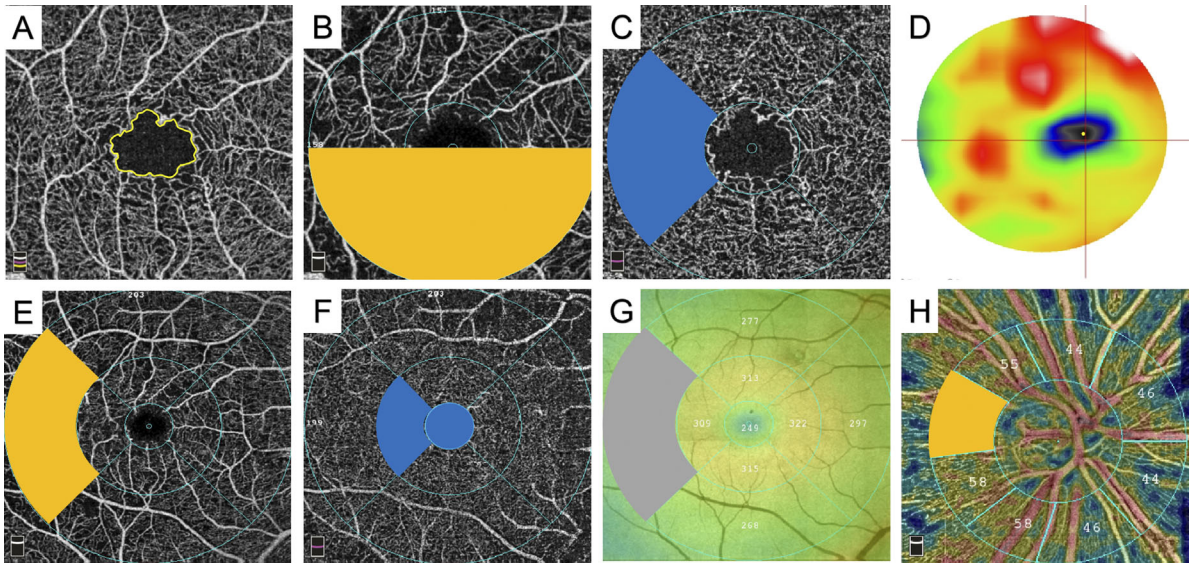

Figure 4. Schematic presentation illustrating the parsimonious parameters in combined blocks on OCTA images at different scans. (**A–C**) A 3.0 mm scan in combination 1. (**A**) FAZ perimeter (*yellow ring*). (**B**) Inferior hemisphere SCP VD (*yellow*). (**C**) Temporal parafoveal DCP VD (*blue*). (**E–G**) A 6.0 mm scan in combination 2. (**E**) Temporal perifoveal SCP VD (*yellow*). (**F**) Foveal and temporal parafoveal DCP VD (*blue*). (**G**) Temporal perifoveal retinal thickness (*gray*). (**D**) GCC scan in combinations 1 and 2. (**H**) Temporal superior peripapillary VD (*yellow*) in 4.5 mm scan in combination 1 and 2.

results were similar to those in patients with DME. In both 3.0 mm and 6.0 mm scans, OCTA parameters were consistent with those in eyes with DME except nasal parafoveal DCP VD and AI (Supplementary Fig. S1A–S1D, S1F–S1I). In 4.5 mm scans, except temporal inferior peripapillary VD and nasal inferior RNFL thickness, decreased temporal superior and nasal inferior peripapillary VD, and increased temporal superior RNFL thickness, were similar to the results in eyes with DME (Supplementary Fig. S1E and S1J). The results of GCC scan were consistent with those in eyes with DME. In

Investigative Ophthalmology & Visual Science

both combinations 1 and 2, OCTA parameters were consistent with those in eyes with DME except temporal parafoveal DCP VD (Supplementary Fig. S2).

Discussion

This study demonstrated retinal microvascular and neural changes in all stages of DR based on different OCTA scan patterns, including retina 3.0 mm, retina 6.0 mm, disc 4.5 mm, and GCC scans. Furthermore, a set of OCTA parameters related to DR severity were identified from numerous parameters of each scanning pattern, including FAZ perimeter; FD-300; temporal perifoveal SCP VD and retinal thickness; temporal and nasal parafoveal DCP VD; peripapillary VD in temporal superior, nasal inferior, and temporal inferior sectors; temporal superior and nasal inferior peripapillary RNFL thickness; GCC thickness; and FLV.

OCTA has been widely considered as an effective tool to diagnose and evaluate DR. However, because of the diversity of scanning patterns and parameters, OCTA generates complicated results and confuses the clinical assessment. Therefore, we used the LASSO regression model to identify sensitive OCTA parameters related to the severity of DR in different scanning patterns. From a total of 116 parameters of four scanning patterns related to retinal VD, retinal thickness, and neural changes, 21 sensitive parameters were identified; furthermore, six and seven sensitive parameters were identified in two combined blocks. The results of this study indicate that identifying and observing these parameters could contribute to a more rapid and an accurate assessment of DR.

Because DR may cause extensive damage to the retinal microvasculature, we examined the ability of the two retinal scanning patterns in OCTA, namely, a 3.0 mm scan and a 6.0 mm scan, to predict the vascular structure alterations in DR. Although the images obtained from both these scanning patterns effectively differentiated early and late stages of DR, their results were not accurately consistent. This discrepancy could be attributed to their different detection sensitivities for different subfields caused by the difference in scanning resolution and range. In a 3.0 mm scan, the sampling density is 304 × 304 and the range is a 3-mm wide area from the fovea; in a 6.0 mm scan, they are 400 × 400 and a 6-mm wide area from the fovea. Because the microvasculature damage of DR usually begins around the macula, and the 3.0 mm scan generates high-quality images in this area, Hirano et al.[4] considered 3.0 mm scan images to be the best for predicting the presence/absence of DR. However, with the progress of retinopathy, the macular damage aggravates and enlarges, and the 6.0 mm scan could thus be more suitable to detect these changes; specifically, in our study it showed significant differences in VD and retinal thickness of temporal perifoveal SCP. Based on previous studies and ours, we postulate 3.0 mm scan to be more appropriate for early DR, and a 6.0 mm scan for advanced DR.

The FAZ is a physiologic and capillary-free area in the center of the macula, which is responsible for epicritic vision and central vision.[26] Previous analyses of the FAZ in DR have indicated an increase in the dimensions of FAZ that is related to disease severity, including area, diameter, perimeter, and AI.[3,5,6,19] Our findings indicate that the significant increase in the FAZ perimeter, enlarged AI, and decreased FD-300 are associated with the DR progression; however, the FAZ area exhibited no significant difference when a set of FAZ parameters were considered simultaneously, suggesting that FAZ becomes more acircular and exhibits a decrease in capillary density with DR progression, which influences the FAZ perimeter, AI, and FD-300, but not the area.[1,14] These changes in the FAZ margin are largely due to capillary dropout, as well as macular vascular remodeling, which causes a decrease in vascular density and perfusion index.[27] The pathologic mechanisms underlying these changes are multifactorial, with capillary occlusion and hemodynamic disorder, such as blood flow reduction,[28] endothelial dysfunctions,[29] and an increase in vascular endothelial growth factor level.[30] After adjusting for age, sex, and AL, this study demonstrates that the FAZ perimeter and the FD-300 in both 3.0 mm and 6.0 mm scans could be good indicators of vascular loss to predict and classify the stage of DR.

The role of VD in vascular abnormalities involved in the macular area has been widely discussed. Recent studies have revealed a reduction in macular VD in the superficial and deep retinal layers in eyes with preclinical DR, early DR, or worsening DR,[1,8,10,12,13,19] suggesting that VD could be one of the most sensitive metrics for diagnosis and monitoring of DR. Further, it has been reported that vascular disorder of DR exhibits a nonuniform distribution within the retina.[31] Moreover, Kaizu et al.[6] indicated that the appearance of spatial biases of macular capillary dropout with the onset of DR, and that the hierarchical bias of VD significantly shifts to a DCP dominance with the progression of DR. In our study, the DCP in macular fovea and parafovea had a low VD, which result is consistent with that of several studies on the deep plexus dominance of DR-related vascular disorders.[6,7] Moreover, we found that SCP in the temporal perifovea exhibits an increase in microvascular dropout, with an increase in the severity of DR. Our findings suggest that the progression of DR differentially affects the SCP and the DCP in different susceptible subfields. Future studies are required to investigate these specific effects.

As a neurodegenerative disease, retinal vascular and optic neuronal damages have already started, even in preclinical DR. In studies related to primary open-angle glaucoma,[16] hypertensive retinopathy,[32] and preclinical or early DR,[5,20–22] a significant decrease in peripapillary VD, peripapillary RNFL thickness, and GCC thickness has been reported. Our study presented similar results for early DR, and further found more sensitive parameters related to the severity of DR, including VD in the temporal superior, nasal inferior, and temporal inferior peripapillary areas; RNFL thickness in temporal superior and nasal inferior areas; GCC thickness; and FLV. However, differing from the case of early DR, the thickness in RNFL and GCC increased with the progression of DR, even in eyes without DME. We speculate that, with the aggravation of retinopathy, nerve cells swelling or even death could result in an increase in RNFL and GCC thickness. Our results reconfirm that the chronic damage induced by hyperglycemia is not only characterized by vascular loss and remodeling in the macular area, but also represented as changes in the disc capillaries and the ganglion cells.

To our knowledge, this study innovatively quantified and compared the microvascular and the neural changes in all stages of DR using OCTA. Because DR is a neurovascular degenerative disease, we consider that the 6.0 mm scan, along with 4.5 mm scan and GCC scan, could be the best scanning pattern to assess the DR severity. The temporal perifoveal SCP VD and retinal thickness, temporal parafoveal and foveal DCP VD, temporal superior peripapillary VD,

Investigative Ophthalmology & Visual Science

GCC thickness, and FLV could be the best parameters to effectively identify and differentiate the severity of DR. However, several limitations are inevitable in this study: one is the limitation of OCTA technology with a macular scanning area, which does not provide the vascular changes in the midperipheral retina. Because the vascular alterations in DR extend beyond the posterior pole, a wide-field OCTA scan such as 12.0 mm pattern could be more useful to evaluate DR. DR pathology may thus be evaluated in greater detail by a combination of OCTA scan patterns and sizes. Another limitation is the number of samples considered in this study. The relatively small number of eyes could have caused the variation in the results of 3.0 mm and 6.0 mm scans, in addition to the difference in scanning resolution and range of these scans.

In conclusion, our study confirmed that DR is a diabetic complication that includes both retinal microvascular impairment and neural changes. After adjusting for age, sex, and AL, we quantified a set of microvascular and neural OCTA parameters related to the severity of DR, which could accurately differentiate the stages of DR. Further studies on ocular and systemic parameters are required to compose and validate an effective model for better screening and evaluation of DR.

Acknowledgments

The authors gratefully thank the Statistics Office, Information and Statistics Center, Guangdong Provincial People's Hospital (Guangdong Academy of Medical Sciences) for excellent statistical assistance in this work.

Supported by the Guangdong Basic and Applied Basic Research Foundation (2017A030313609, 2019A1515010697); and the Project of the Guangdong Medical Science and Technology Research Foundation, Guangzhou, China (A2018401, A2019380). The funding organizations had no role in the design or conduct of this research.

Disclosure: **X. Li,** None; **J. Xie,** None; **L. Zhang,** None; **Y. Cui,** None; **G. Zhang,** None; **X. Chen,** None; **J. Wang,** None; **A. Zhang,** None; **T. Huang,** None; **Q. Meng,** None

References

1. Bhanushali D, Anegondi N, Gadde SG, et al. Linking retinal microvasculature features with severity of diabetic retinopathy using optical coherence tomography angiography. *Invest Ophthalmol Vis Sci*. 2016;57:519–525.
2. Samara WA, Shahlaee A, Adam MK, et al. Quantification of diabetic macular ischemia using optical coherence tomography angiography and its relationship with visual acuity. *Ophthalmology*. 2017;124:235–244.
3. Lu Y, Simonett JM, Wang J, et al. Evaluation of automatically quantified foveal avascular zone metrics for diagnosis of diabetic retinopathy using optical coherence tomography angiography. *Invest Ophthalmol Vis Sci*. 2018;59:2212–2221.
4. Hirano T, Kitahara J, Toriyama Y, Kasamatsu H, Murata T, Sadda S. Quantifying vascular density and morphology using different swept-source optical coherence tomography angiographic scan patterns in diabetic retinopathy. *Br J Ophthalmol*. 2019;103:216–221.
5. Kim K, Kim ES, Yu SY. Optical coherence tomography angiography analysis of foveal microvascular changes and inner retinal layer thinning in patients with diabetes. *Br J Ophthalmol*. 2018;102:1226–1231.
6. Kaizu Y, Nakao S, Yoshida S, et al. Optical coherence tomography angiography reveals spatial bias of macular capillary dropout in diabetic retinopathy. *Invest Ophthalmol Vis Sci*. 2017;58:4889–4897.
7. Chen Q, Ma Q, Wu C, et al. Macular vascular fractal dimension in the deep capillary layer as early indicator of microvascular loss for retinopathy in type 2 diabetic patients. *Invest Ophthalmol Vis Sci*. 2017;58:3785–3794.
8. Schottenhamml J, Moult EM, Ploner S, et al. An automatic, intercapillary area-based algorithm for quantifying diabetes related capillary dropout using optical coherence tomography angiography. *Retina*. 2016;36:93–101.
9. Salz DA, de Carlo TE, Adhi M, et al. Select features of diabetic retinopathy on swept-source optical coherence tomography angiography compared with fluorescein angiography and normal eyes. *JAMA Ophthalmol*. 2016;134:644–650.
10. Ashraf M, Nesper PL, Jampol M, Yu F, Fawzi AA, et al. Statistical model of optical coherence tomography angiography parameters that correlate with severity of diabetic retinopathy. *Invest Ophthalmol Vis Sci*. 2018;59:4292–4298.
11. Takase N, Nozaki M, Kato A, Ozeki H, Yoshida M, Ogura Y. Enlargement of foveal avascular zone in diabetic eyes evaluated by en face optical coherence tomography angiography. *Retina*. 2015;35:2377–2383.
12. Zahid S, Dolz-Marco R, Freund KB, et al. Fractal dimensional analysis of optical coherence tomography angiography in eyes with diabetic retinopathy. *Invest Ophthalmol Vis Sci*. 2016;57:4940–4947.
13. Sandhu HS, Eladawi N, Elmogy M, et al. Automated diabetic retinopathy detection using optical coherence tomography angiography: a pilot study. *Br J Ophthalmol*. 2018;102:1564–1569.
14. Krawitz BD, Mo S, Geyman LS, et al. Acircularity index and axis ratio of the foveal avascular zone in diabetic eyes and healthy controls measured by optical coherence tomography angiography. *Vision Res*. 2017;139:177–186.
15. Bhardwaj S, Tsui E, Zahid S, et al. Value of fractal analysis of optical coherence tomography angiography in various stages of diabetic retinopathy. *Retina*. 2018;38:1816–1823.
16. Alnawaiseh M, Lahme L, Muller V, Rosentreter A, Eter N. Correlation of flow density, as measured using optical coherence tomography angiography, with structural and functional parameters in glaucoma patients. *Graefes Arch Clin Exp Ophthalmol*. 2018;256:589–597.
17. Li Z, Wen X, Zeng P, et al. Do microvascular changes occur preceding neural impairment in early stage diabetic retinopathy? Evidence based on the optic nerve head using optical coherence tomography angiography. *Acta Diabetol*. 2019; 56:531–539.
18. Pusparajah P, Lee LH, Abdul Kadir K. Molecular markers of diabetic retinopathy: potential screening tool of the future? *Front Physiol*. 2016;7:200.
19. Li Z, Alzogool M, Xiao J, Zhang S, Zeng P, Lan Y. Optical coherence tomography angiography finding of neurovascular changes in type 2 diabetes mellitus without clinical diabetic retinopathy. *Acta Diabetol*. 2018;55:1075–1082.
20. Vujosevic S, Muraca A, Alkabes M, et al. Early microvascular and neural changes in patients with type 1 and type 2 diabetes mellitus without clinical signs of diabetic retinopathy. *Retina*. 2019;39:435–445.
21. Vujosevic S, Midena E. Retinal layers changes in human preclinical and early clinical diabetic retinopathy support early retinal neuronal and Müller cells alterations. *J Diabetes Res*. 2013;2013:905058.
22. van Dijk HW, Verbraak FD, Kok PH, et al. Early neurodegeneration in the retina of type 2 diabetic patients. *Invest Ophthalmol Vis Sci*. 2012;53:2715–2719.

23. Solomon SD, Chew E, Duh EJ, et al. Diabetic retinopathy: a position statement by the American Diabetes Association. *Diabetes Care*. 2017;40:412–418.
24. Wilkinson CP, Ferris FL, et al. Proposed international clinical diabetic retinopathy and diabetic macular edema disease severity scales. *Ophthalmology*. 2003;110:1677–1682.
25. Jia Y, Tan O, Tokayer J, et al. Split-spectrum amplitude-decorrelation angiography with optical coherence tomography. *Opt Exp*. 2012;20: 4710–4725.
26. Engerman RL. Development of the macular circulation. *Invest Ophthalmol Vis Sci*. 1976;15:835–840.
27. Sasongko MB, Wong TY, Nguyen TT, Cheung CY, Shaw JE, Wang JJ. Retinal vascular tortuosity in person with diabetes and diabetic retinopathy. *Diabetologia*. 2011;54:2409–2416.
28. Kristinsson JK, Gottfredsdottir MS, Stefansson E. Retinal vessel dilatation and elongation precedes diabetic macular edema. *Br J Ophthalmol*. 1997;81:274–278.
29. Witt N, Wong TY, Hughes AD, et al. Abnormalities of retinal microvascular structure and risk of mortality from ischemic heart disease and stroke. *Hypertension*. 2006;47:975–981.
30. Hartnett ME, Martiniuk D, Byfield G, Geisen P, Zeng G, Bautch VL. Neutralizing VEGF decreases tortuosity and alters endothelial cell division orientation in arterioles and veins in a rat model of ROP: relevance to plus disease. *Invest Ophthalmol Vis Sci*. 2008;49:3017–3114.
31. Talor E, Dobree JH. Proliferative diabetic retinopathy. Site and size of initial lesions. *Br J Ophthalmol*. 1970;54:11–18.
32. Lim HB, Lee MW, Park JH, Kim K, Jo YJ, Kim JY. Changes in ganglion cell-inner plexiform layer thickness and retinal microvasculature in hypertension: an OCTA study. *Am J Ophthalmol*. 2019;199:167–176.

Investigative Ophthalmology & Visual Science